

Dear Prof. Tian,

Thank you for your decision letter on our manuscript entitled “Accelerated hydrological cycle over the Sanjiangyuan region induces more streamflow extremes at different global warming levels”. We have carefully considered your suggestion, and proofread and edited the English. We hope that you find the revised manuscript and the response acceptable to *HESS*. Your comments are italicized and our responses immediately follow.

We appreciate the effort you spent to process the manuscript and look forward to hearing from you soon.

Sincerely yours,

Xing Yuan

I suggest the authors to double check details of the manuscript and improve the language. I made some comments along my reading, which did absolutely not covering all of them.

Response: Thanks for the suggestion. We have double checked the manuscript and edited the English carefully, including making the statement clearer, adding the equation numbers on the right-hand side, changing the tense and revising the grammar mistakes. Detailed information is shown below:

1. Change “... changes in streamflow extremes ...” to “... changes of streamflow extremes ...” L19
2. Change “The response of regional and global terrestrial hydrological processes, including streamflow and its extremes, to ...” to “The response of regional and global terrestrial hydrological processes (e.g., streamflow and its extremes) to ...” L48-50
3. Change “... because the increased CO₂ concentration will decrease the vegetation transpiration by reducing the stomatal conductance” to “... through decreasing the stomatal conductance and vegetation transpiration” L57-58
4. Change “... have a significant role in ...” to “... play a significant role in ...” L61
5. Change “... whether their combined impact changes at different warming levels ...” to “... whether their combined impact differs among different warming levels ...” L65-66

6. Change “Changes in streamflow and its extremes ... not only influence the local ecosystems..., but also affect the security of food...” to “Changes of streamflow and its extremes ... not only influence the local ecosystems ..., but also the security of food...” L69-71
7. Change “This makes it difficult to assess the ... on this vital headwaters region” to “Solving the above issues is essential for assessing the ... on this vital headwaters region.” L95-96
8. Change “In this study, we investigate the ...” to “In this study, we investigated the ...” L97
9. Change “The combined impacts of ... are also quantified” to “The combined impacts of ... were also quantified” L100
10. Change “Monthly terrestrial water storage change observation and its uncertainty ... was provided ...” to “Estimations of monthly terrestrial water storage change and its uncertainty ... were provided ...” L118-120
11. Change “... were also used to evaluate the model performance on ET simulation.” to “... were used to evaluate the ET simulation.” L125-126
12. Change “(CMFD) is taken as meteorological observation” to “(CMFD) was taken as meteorological observation” L150
13. Change “the influences of soil organic matters on soil hydrological properties were incorporated into ...” to “... the hydrological properties of soil organic matters were incorporated into ...” L177-178
14. Add equation numbers. L185, 201-203, 240, 246
15. Change “were calculated for the observed and simulated ..., to evaluate the model performance.” to “were calculated for validating the simulated ...” L196-198
16. Change “... are observed and simulated standard deviations respectively” to “... are standard deviations for observed and simulated variables respectively” L206-207
17. Change “Compared with the observation at Tangnaihahi (TNH) and Zhimenda (ZMD) stations, the Kling-Gupta efficiencies of the CMFD/CSSPv2 simulated monthly streamflow are 0.94 and 0.91 respectively.” to “The Kling-Gupta efficiencies of CMFD/CSSPv2 simulated monthly streamflow are 0.94 and 0.91 over Tangnaihahi (TNH) and Zhimenda (ZMD) stations, respectively.” L279-281
18. Change “by large uncertainty in the changes during summer and autumn seasons.” to “by large uncertain changes during summer and autumn seasons.” L308-309
19. Change “a left shift of PDF for P-ET.” to “... a left shift for the PDF of P-ET.”

L346-347

20. Change “shows little change to the right tails in the PDF” to “shows little change in the right tails of the PDF” L355

21. Change “as the increased LAI enhancement on ET is weaker than the suppression effect of CO₂ physiological forcing” to “as enhancement effect of the increased LAI on ET is weaker than the suppression effect of CO₂ physiological forcing” L373-375

22. Change “the robust of the result” to “the robustness of the result” L442

L40, check the number

Response: Thanks for the suggestion. We have revised as “0.17°C/decade” and double checked the number according to the reference. Moreover, other numbers are also rechecked.

L50-51, are these references research papers or review articles? Suggest to provide several most recent review papers.

Response: We have added the IPCC special report on the 1.5°C warming that reviewed previous works comprehensively (Hoegh-Guldberg et al., 2018), as well as a recent paper (Xu et al., 2019) to the reference list. We still keep some representative research papers. The references are now: “(Döll et al., 2018; Hoegh-Guldberg et al., 2018; Marx et al., 2018; Mohammed et al., 2017; Thober et al., 2018; Xu et al., 2019; Zhang et al., 2016)” L50-52

L77, where is this example?

Response: The example is the work that investigated the influences of climate change and ecological change on the streamflow. We have revised the statement to avoid misunderstanding: “... Historical changes of climate and ecology (e.g., land cover) are found to cause significant reduction in mean and high flows over the Yellow River headwaters during 1979-2005, which potentially increases drought risk over its downstream areas (Ji and Yuan, 2018). And the CO₂ physiological forcing is revealed to cause equally large changes in regional flood extremes as the precipitation over the Yangtze and Mekong rivers (Fowler et al., 2019). Thus the Sanjiangyuan region is a sound region to investigate the role of climate change and ecological change ...” L75-83

L228, need an equation to define SSI, which is important for understanding

Response: Thanks for the suggestion. We have added equations and described the calculation of SSI in details.

“In this research, the standardized streamflow index (SSI) was used to define dry and wet extremes (Vicente-Serrano et al., 2012; Yuan et al., 2017). The July-August-September (JAS) mean streamflow for each year of the reference period was first collected and used to fit a gamma distribution:

$$f(x, \beta, \alpha) = \frac{\beta^\alpha}{\Gamma(\alpha)} x^{\alpha-1} e^{-\beta x} \quad (5)$$

where x means streamflow while α and β are parameters. Then the fitted distribution was used to standardize the JAS mean streamflow in each year (i) during both the reference and projection periods as:

$$\begin{aligned} SSI_i &= Z^{-1}(F(x_i)) \\ F(x_i) &= \int_0^{x_i} f(x, \beta, \alpha) dx \end{aligned} \quad (6)$$

where Z^{-1} means the inverse cumulative distribution function of the normal distribution, while $F(x)$ is the cumulative distribution function of the gamma distribution. Here, dry and wet extremes were defined as SSIs smaller than -1.28 (a probability of 10%) and larger than 1.28 respectively.” L236-250

L428, change “Robust” to “Robustness”

Response: Done as suggested.

Figure 1, legend looks different from the Figure lines(e) says CO2 in north hemisphere, while text says in Sanjiangyuan. Check it.

Response: Thanks for the suggestion. In this study, we did not use gridded CO2 concentration data due to large uncertainty (and very limited heterogeneity) at regional scale. Instead, we used the CO2 concentration averaged over the North Hemisphere to force the offline simulation over the Sanjiangyuan region (i.e., the CO2 concentrations are the same for each grid cell), which is also widely used in many impact studies. We have revised the figure and its caption as follows:

“... (b)-(d) The time series of annual temperature, precipitation, and growing season leaf area index averaged over the Sanjiangyuan region during 1979-2100. (e) Observed and simulated annual CO₂ concentration over the Sanjiangyuan region. ...”

L643-646

1 **Accelerated hydrological cycle over the Sanjiangyuan region induces**
2 **more streamflow extremes at different global warming levels**

3

4 Peng Ji^{1,2}, Xing Yuan^{3*}, Feng Ma³, Ming Pan⁴

5

6 ¹Key Laboratory of Regional Climate-Environment for Temperate East Asia, Institute
7 of Atmospheric Physics, Chinese Academy of Sciences, Beijing 100029, China

8 ²College of Earth and Planetary Sciences, University of Chinese Academy of Sciences,
9 Beijing 1000493, China

10 ³School of Hydrology and Water Resources, Nanjing University of Information
11 Science and Technology, Nanjing 210044, China

12 ⁴Department of Civil and Environmental Engineering, Princeton University, Princeton,
13 New Jersey, USA

14

15 **Correspondence to: Xing Yuan (xyuan@nuist.edu.cn)*

16 **Abstract.** Serving source water for the Yellow, Yangtze and Lancang-Mekong rivers,
17 the Sanjiangyuan region concerns 700 million people over its downstream areas.
18 Recent research suggests that the Sanjiangyuan region will become wetter in a
19 warming future, but future changes [in](#)of streamflow extremes remain unclear due to
20 the complex hydrological processes over high-land areas and limited knowledge of
21 the influences of land cover change and CO₂ physiological forcing. Based on high
22 resolution land surface modeling during 1979~2100 driven by the climate and
23 ecological projections from 11 newly released Coupled Model Intercomparison
24 Project Phase 6 (CMIP6) climate models, we show that different accelerating rates of
25 precipitation and evapotranspiration at 1.5°C global warming level induce 55% more
26 dry extremes over Yellow river and 138% more wet extremes over Yangtze river
27 headwaters compared with the reference period (1985~2014). An additional 0.5°C
28 warming leads to a further nonlinear and more significant increase for both dry
29 extremes over Yellow river (22%) and wet extremes over Yangtze river (64%). The
30 combined role of CO₂ physiological forcing and vegetation greening, which used to
31 be neglected in hydrological projections, is found to alleviate dry extremes at 1.5 and
32 2.0°C warming levels but to intensify dry extremes at 3.0°C warming level. Moreover,
33 vegetation greening contributes half of the differences between 1.5 and 3.0°C
34 warming levels. This study emphasizes the importance of ecological processes in
35 determining future changes in streamflow extremes, and suggests a “dry gets drier,
36 wet gets wetter” condition over [the warming](#) headwaters.

37 **Keywords** Terrestrial hydrological cycle, streamflow extremes, global warming levels,

39 1 Introduction

40 Global temperature has increased at a rate of [0.17°C/decade](#) since 1970,
41 contrary to the cooling trend over the past 8000 years (Marcott et al., 2013). The
42 temperature measurements suggest that 2015-2019 is the warmest five years and
43 2010-2019 is also the warmest decade since 1850 (WMO, 2020). To mitigate the
44 impact of this unprecedented warming on the global environment and human society,
45 195 nations adopted the Paris Agreement which decides to “hold the increase in the
46 global average temperature to well below 2°C above pre-industrial levels and pursuing
47 efforts to limit the temperature increase to 1.5°C”.

48 The response of regional and global terrestrial hydrological processes, [including](#)
49 [\(e.g., streamflow and its extremes\)](#); to different global warming levels has been
50 investigated by numerous studies in recent years ([Chen et al., 2017](#); Döll et al., 2018;
51 [Hoegh-Guldberg et al., 2018](#); Marx et al., 2018; Mohammed et al., 2017; Thober et al.,
52 2018; [Xu et al., 2019](#); Zhang et al., 2016). In addition to climate change, recent works
53 reveal the importance of the ecological factors (e.g., the CO₂ physiological forcing
54 and land cover change), which are often unaccounted for in hydrological modeling
55 works, in modulating the streamflow and its extremes. For example, the increasing
56 CO₂ concentration is found to alleviate the decreasing trend of streamflow in the
57 future at global scale, ~~because the increased CO₂ concentration will through~~
58 ~~decrease~~ [the stomatal conductance and](#) vegetation transpiration ~~by reducing the~~
59 ~~stomatal conductance~~ (known as the CO₂ physiological forcing) (Fowler et al., 2019;
60 Wiltshire et al., 2013; Yang et al., 2019; Zhu et al., 2012). Contrary to the CO₂

61 physiological forcing, the vegetation greening in a warming climate is found to
62 [haveplay](#) a significant role in exacerbating hydrological drought, as it enhances
63 transpiration and dries up the land (Yuan et al., 2018b). However, the relative
64 contributions of CO₂ physiological forcing and vegetation greening to the changes in
65 terrestrial hydrology especially the streamflow extremes are still unknown, and
66 whether their combined impact [changesdiffers atamong](#) different warming levels
67 needs to be investigated.

68 Hosting the headwaters of the Yellow river, the Yangtze river and the
69 Lancang-Mekong river, the Sanjiangyuan region is known as the “Asian Water
70 Tower” and concerns 700 million people over its downstream areas. Changes [inof](#)
71 streamflow and its extremes over the Sanjiangyuan region not only influence the local
72 ecosystems, environment and water resources, but also [affect](#) the security of food,
73 energy, and water over the downstream areas. Both the regional climate and
74 ecosystems show significant changes over the Sanjiangyuan region due to global
75 warming (Bibi et al., 2018; Kuang and Jiao, 2016; Liang et al., 2013; Yang et al., 2013;
76 Zhu et al., 2016).; [Historical changes of climate and ecology \(e.g. land cover\) are
77 found to cause significant reduction in mean and high flows over the Yellow River
78 headwaters during 1979-2005, which potentially increases drought risk over its
79 downstream areas \(Ji and Yuan, 2018\). And the CO₂ physiological forcing is revealed
80 to cause equally large changes in regional flood extremes as the precipitation over the
81 Yangtze and Mekong rivers \(Fowler et al., 2019\). which makes it aThus the
82 Sanjiangyuan region is a](#) sound region to investigate the role of climate change and

83 ecological change (e.g., land cover change and CO₂ physiological forcing) in
84 influencing the streamflow and its extremes (Cuo et al., 2014; Ji and Yuan, 2018; Zhu
85 et al., 2013). ~~For example, historical changes in climate and ecology (e.g. land cover)~~
86 ~~are found to cause significant reduction in mean and high flows during 1979-2005,~~
87 ~~which potentially increases drought risk over its downstream areas (Ji and Yuan,~~
88 ~~2018). And the CO₂ physiological forcing is revealed to cause equally large changes in~~
89 ~~regional flood extremes as the precipitation over the Yangtze and Mekong rivers~~
90 ~~(Fowler et al., 2019).~~ Recent research suggests that the Sanjiangyuan region will
91 become warmer and wetter in the future, and extreme precipitation will also increase
92 at the 1.5°C global warming level and further intensify with a 0.5°C additional
93 warming (Li et al., 2018; Zhao et al., 2019). However, how the streamflow extremes
94 would respond to the 1.5°C warming, what an additional 0.5°C or even greater
95 warming would cause, and how much contributions do the ecological factors (e.g.,
96 CO₂ physiological forcing and land cover change) have, are still unknown. ~~This~~
97 ~~makes it difficult~~ Solving the above issues is essential for ~~to~~-assessing the climate and
98 ecological impact on this vital headwaters region.

99 In this study, we investigated the future changes in the streamflow extremes over
100 the Sanjiangyuan region from an integrated eco-hydrological perspective by taking
101 CO₂ physiological forcing and land cover change into consideration. The combined
102 impacts of the above two ecological factors at different global warming levels ~~are~~were
103 also quantified and compared with the impact of climate change. The results will help
104 understand the role of ecological factors in future terrestrial hydrological changes

105 over the headwater regions like the Sanjiangyuan, and provide guidance and support
106 for the stakeholders to make relevant decisions and plans.

107 **2 Data and methods**

108 **2.1 Study domain and observational data**

109 The Sanjiangyuan region is located at the eastern part of the Tibetan Plateau
110 (Figure 1a), with the total area and mean elevation being 3.61×10^5 km² and 5000 m
111 respectively. It plays a critical role in providing freshwater, by contributing 35%, 20%
112 and 8% to the total annual streamflow of the Yellow, Yangtze and Lancang-Mekong
113 rivers (Li et al., 2017; Liang et al., 2013). The source regions of Yellow, Yangtze and
114 Lancang-Mekong rivers account for 46%, 44% and 10% of the total area of the
115 Sanjiangyuan individually, and the Yellow river source region has a warmer climate
116 and sparser snow cover than the Yangtze river source region.

117 Monthly streamflow observations from the Tangnaihai (TNH) and the Zhimenda
118 (ZMD) hydrological stations (Figure 1a), which were provided by the local authorities,
119 were used to evaluate the streamflow simulations. Data periods are 1979-2011 and
120 1980-2008 for the Tangnaihai and Zhimenda stations individually. [Estimations of](#)
121 [m](#)Monthly terrestrial water storage change ~~observation~~ and its uncertainty during
122 2003-2014 [wasere](#) provided by the Jet Propulsion Laboratory (JPL), which used the
123 mass concentration blocks (mascons) basis functions to fit the Gravity Recovery and
124 Climate Experiment (GRACE) satellite's inter-satellite ranging observations (Watkins
125 et al., 2015). The Model Tree Ensemble evapotranspiration (MTE_ET; Jung et al.,
126 2009) and the Global Land Evaporation Amsterdam Model evapotranspiration

127 (GLEAM_ET) version 3.3a (Martens et al., 2017) were ~~also~~ used to evaluate the
128 ~~model performance on~~ ET simulation.

129 2.2 CMIP6 Data

130 Here, 19 Coupled Model Intercomparison Project phase 6 (CMIP6, Eyring et al.,
131 2016) models which provide precipitation, near-surface temperature, specific
132 humidity, 10-m wind speed, surface downward shortwave and longwave radiations at
133 daily timescale were first selected for evaluation. Then, models were chosen for the
134 analysis when the simulated meteorological forcings (e.g., precipitation, temperature,
135 humidity, and shortwave radiation) averaged over the Sanjiangyuan region have the
136 same trend signs as the observations during 1979-2014. Table 1 shows the 11 CMIP6
137 models that were finally chosen in this study. For the future projection (2015-2100),
138 we chose two Shared Socioeconomic Pathways (SSP) experiments: SSP585 and
139 SSP245. SSP585 combines the fossil-fueled development socioeconomic pathway
140 and 8.5W/m² forcing pathway (RCP8.5), while SSP245 combines the moderate
141 development socioeconomic pathway and 4.5 W/m² forcing pathway (RCP4.5)
142 (O'Neill et al., 2016). Land cover change is quantified by leaf area index (LAI) as
143 there is no significant transition between different vegetation types (not shown)
144 according to the Land-use Harmonization 2 (LUH2) dataset
145 (<https://esgf-node.llnl.gov/search/input4mips/>). For the CNRM-CM6-1, FGOALS-g3
146 and CESM2, the ensemble mean of LAI simulations from the other 8 CMIP6 models
147 was used because CNRM-CM6-1 and FGOALS-g3 do not provide dynamic LAI
148 while the CESM2 simulates an abnormally large LAI over the Sanjiangyuan region.

149 To avoid systematic bias in meteorological forcing, the trend-preserved bias
150 correction method suggested by ISI-MIP (Hempel et al., 2013), was applied to the
151 CMIP6 model simulations at monthly scale. The China Meteorological Forcing
152 Dataset (CMFD) [iswas](#) taken as meteorological observation (He et al., 2020). For
153 each month, temperature bias in CMIP6 simulations during 1979-2014 was directly
154 deducted. Future temperature simulations in SSP245 and SSP585 experiments were
155 also adjusted according to the historical bias. Other variables were corrected by using
156 a multiplicative factor, which was calculated by using observations to divide
157 simulation during 1979-2014. In addition, monthly leaf area index was also adjusted
158 to be consistent with satellite observation using the same method as temperature. All
159 variables were first interpolated to the 10 km resolution over the Sanjiangyuan region
160 and the bias correction was performed for each CMIP6 model at each grid. After bias
161 correction, absolute changes of temperature and leaf area index, and relative changes
162 of other variables were preserved at monthly time scale (Hempel et al., 2013). Then,
163 the adjusted CMIP6 daily meteorological forcings were disaggregated into hourly
164 using the diurnal cycle ratios from the China Meteorological Forcing Dataset.

165 The historical CO₂ concentration used here is the same as the CMIP6 historical
166 experiment (Meinshausen et al., 2017), while future CO₂ concentration in SSP245 and
167 SSP585 scenarios came from simulations of a reduced-complexity carbon-cycle
168 model MAGICC7.0 (Meinshausen et al., 2020).

169 **2.3 Experimental design**

170 The land surface model used in this study is the Conjunctive Surface-Subsurface

171 Process model version 2 (CSSPv2), which has been proved to simulate the energy and
 172 water processes over the Sanjiangyuan region well (Yuan et al., 2018a). Figure 2
 173 shows the structure and main ecohydrological processes in CSSPv2. The CSSPv2 is
 174 rooted in the Common Land Model (CoLM; Dai et al., 2003) with some
 175 improvements at hydrological processes. CSSPv2 has a volume-averaged soil
 176 moisture transport (VAST) model, which solves the quasi-three dimensional
 177 transportation of the soil water and explicitly considers the variability of moisture flux
 178 due to subgrid topographic variations (Choi et al., 2007). Moreover, the Variable
 179 Infiltration Capacity runoff scheme (Liang et al., 1994), and the [hydrological](#)
 180 [properties](#) influences of soil organic matters ~~on soil hydrological properties~~ were
 181 incorporated into the CSSPv2 by Yuan et al. (2018a), to improve its performance in
 182 simulating the terrestrial hydrology over the Sanjiangyuan region. Similar to CoLM
 183 and Community Land Model (Oleson et al., 2013), vegetation transpiration in
 184 CSSPv2 is based on Monin-Obukhov similarity theory, and the transpiration rate is
 185 constrained by leaf boundary layer and stomatal conductances. Parameterization of
 186 the stomatal conductance (g_s) in CSSPv2 is

$$187 \quad g_s = m \frac{A_n}{\frac{P_{CO_2}}{P_{atm}}} h_s + b\beta_t \quad (1)$$

188 where the m is a plant functional type dependent parameter, A_n is leaf net
 189 photosynthesis ($\mu mol CO_2 m^{-2} s^{-1}$), P_{CO_2} is the CO_2 partial pressure at the leaf
 190 surface (Pa), P_{atm} is the atmospheric pressure (Pa), h_s is the leaf surface
 191 humidity, b is the minimum stomatal conductance ($\mu mol m^{-2} s^{-1}$), while β_t is the
 192 soil water stress function. Generally, the stomatal conductance decreases with the

193 increasing of CO₂ concentration.

194 First, bias-corrected meteorological forcings from CMIP6 historical experiment
195 were used to drive the CSSPv2 model (CMIP6_His/CSSPv2). All simulations were
196 conducted for two cycles during 1979-2014 at half-hourly time step and 10 km spatial
197 resolution, with the first cycle serving as the spin-up. Correlation coefficient (CC) and
198 root mean squared error (RMSE) were calculated for validating the observed and
199 simulated monthly streamflow, annual evapotranspiration and monthly terrestrial
200 water storage, to evaluate the model performance. The King-Gupta efficiency (KGE;
201 Gupta et al., 2009), which is widely used in streamflow evaluations, was also
202 calculated. Above metrics were calculated as follows:

$$203 \quad \text{CC} = \frac{\sum_{i=1}^n (x_i - \bar{x})(y_i - \bar{y})}{\sqrt{\sum_{i=1}^n (x_i - \bar{x})^2 \sum_{i=1}^n (y_i - \bar{y})^2}} \quad (2)$$

$$204 \quad \text{RMSE} = \sqrt{\frac{\sum_{i=1}^n (x_i - y_i)^2}{n}} \quad (3)$$

$$205 \quad \text{KGE} = 1 - \sqrt{(1 - \text{CC})^2 + (1 - \frac{\sigma_x}{\sigma_y})^2 + (1 - \frac{\bar{x}}{\bar{y}})^2} \quad (4)$$

206 where x_i and y_i are observed and simulated variables in a specific month/year i
207 individually, and \bar{x} and \bar{y} are the corresponding monthly/annual means during the
208 whole evaluation period n . The σ_x and σ_y are observed and simulated standard
209 deviations for observed and simulated variables respectively. The correlation
210 coefficient represents the correlation between simulation and observation, while
211 RMSE means simulated error. The KGE ranges from negative infinity to 1, and model

212 simulations can be regard as satisfactory when the KGE is larger than 0.5 (Moriassi et
213 al., 2007).

214 Second, bias-corrected meteorological forcings in SSP245 and SSP585 were
215 used to drive CSSPv2 during 2015-2100 with dynamic LAI and CO₂ concentration
216 (CMIP6_SSP/CSSPv2). Initial conditions of CMIP6_SSP/CSSPv2 came from the last
217 year in CMIP6_His/CSSPv2.

218 Then, the second step was repeated twice by fixing the monthly LAI
219 (CMIP6_SSP/CSSPv2_FixLAI) and mean CO₂ concentration
220 (CMIP6_SSP/CSSPv2_FixCO₂) at 2014 level. The difference between
221 CMIP6_SSP/CSSPv2 and CMIP6_SSP/CSSPv2_FixLAI is regarded as the net effect
222 of land cover change, and the difference between CMIP6_SSP/CSSPv2 and
223 CMIP6_SSP/CSSPv2_FixCO₂ is regarded as the net effect of CO₂ physiological
224 forcing.

225 **2.4 Warming level determination**

226 A widely used time-sampling method was adopted to determine the periods of
227 different global warming levels (Chen et al., 2017; Döll et al., 2018; Marx et al., 2018;
228 Mohammed et al., 2017; Thober et al., 2018). According to the HadCRUT4 dataset
229 (Morice et al., 2012), the global mean surface temperature has increased by 0.66°C
230 from the pre-industrial era (1850-1900) to the reference period defined as 1985-2014.
231 Then, starting from 2015, 30-years running mean global temperatures were compared
232 to those of the 1985-2014 period for each GCM simulation. And the
233 1.5°C/2.0°C/3.0°C warming period is defined as the 30-years period when the

234 0.84°C/1.34°C/2.34°C global warming, compared with the reference period
 235 (1985-2014), is first reached. The median years of identified 30-year periods, referred
 236 as “crossing years”, are shown in Table 2.

237 2.5 Definition of dry and wet extremes and robustness assessment

238 In this research, the standardized streamflow index (SSI) was used to define dry
 239 and wet extremes (Vicente-Serrano et al., 2012; Yuan et al., 2017). The
 240 July-August-September (JAS) mean streamflow for each year of the reference period
 241 was first collected and used to fit a gamma distribution:-

$$242 \quad \text{-----} \quad f(x, \beta, \alpha) = \frac{\beta^\alpha}{\Gamma(\alpha)} x^{\alpha-1} e^{-\beta x} \quad (5)$$

243 where x means streamflow, while α and β are parameters~~was first fitted~~
 244 ~~using July-September (flood season) mean streamflow during the reference period.~~
 245 Then the fitted distribution was used to ~~calculate the~~ standardized deviation of the
 246 ~~JAS~~July-September mean streamflow (i.e. SSI) in each year (i) during both the
 247 reference and projection periods as:-

$$248 \quad \text{-----} \quad \begin{aligned} SSI_i &= Z^{-1}(F(x_i)) \\ F(x_i) &= \int_0^{x_i} f(x, \beta, \alpha) dx \end{aligned} \quad (6)$$

249 where Z^{-1} means the inverse cumulative distribution function of the normal
 250 distribution, while $F(x)$ is the cumulative distribution function of the gamma
 251 distribution. Here, dry and wet extremes were defined as ~~where~~SSIs ~~are~~ smaller than
 252 -1.28 (a probability of 10%) and larger than 1.28 respectively.

253 The relative changes in frequency of dry/wet extremes between the reference
 254 period and different warming periods were first calculated for each GCM under each

255 SSP scenario, and the ensemble means were then determined for each warming level.
256 To quantify the uncertainty, the above calculations were repeated by using the
257 bootstrap 10,000 times, and 11 GCMs were resampled with replacement during each
258 bootstrap (Christopher et al., 2018). The 5% and 95% percentiles of the total 10,000
259 estimations were finally taken as the 5~95% uncertainty ranges.

260 **3 Results**

261 **3.1 Terrestrial hydrological changes at different warming levels**

262 As shown in Figures 1b-1e, observations (pink lines) show that the annual
263 temperature, precipitation and growing season LAI increase at the rates of
264 $0.63^{\circ}\text{C}/\text{decade}$ ($p=0$), $16.9 \text{ mm}/\text{decade}$ ($p=0.02$), and $0.02 \text{ m}^2/\text{m}^2/\text{decade}$ ($p=0.001$)
265 during 1979-2014 respectively. The ensemble means of CMIP6 simulations (black
266 lines) can generally capture the historical increasing trends of temperature
267 ($0.30 \text{ }^{\circ}\text{C}/\text{decade}$, $p=0$), precipitation ($7.1 \text{ mm}/\text{decade}$, $p=0$) and growing season LAI
268 ($0.029 \text{ m}^2/\text{m}^2/\text{decade}$, $p=0$), although the trends for precipitation and temperature are
269 underestimated. In 2015-2100, the SSP245 scenario (blue lines) shows continued
270 warming, wetting and greening trends, and the trends are larger in the SSP585
271 scenario (red lines). The CO_2 concentration also keeps increasing during 2015-2100
272 and reaches to 600 ppm and 1150 ppm in 2100 for the SSP245 and SSP585 scenarios
273 respectively. Although the SSP585 scenario reaches the same warming levels earlier
274 than the SSP245 scenario (Table 2), there is no significant difference between them in
275 the meteorological variables during the same warming period (not shown). Thus, we
276 do not distinguish SSP245 and SSP585 scenarios at the same warming level in the

277 following analysis.

278 Figure 3 and Table 3 show the evaluation of model simulation. Driven by
279 observed meteorological and ecological forcings, the CMFD/CSSPv2 simulates
280 monthly streamflow over the Yellow and Yangtze river headwaters quite well.
281 ~~Compared with the observation at Tangnaihai (TNH) and Zhimenda (ZMD) stations,~~
282 ~~€~~The Kling-Gupta efficiencies of ~~the~~ CMFD/CSSPv2 simulated monthly streamflow
283 are 0.94 and 0.91 over Tangnaihai (TNH) and Zhimenda (ZMD) stations, respectively.
284 The simulated monthly Terrestrial Water Storage Anomaly (TWSA) during
285 2003-2014 in CMFD/CSSPv2 also agrees with the GRACE satellite observation and
286 captures the increasing trend. For the interannual variations of evapotranspiration,
287 CMFD/CSSPv2 is consistent with the ensemble mean of the GLEAM_ET and
288 MTE_ET products, and the correlation coefficient and root mean squared error
289 (RMSE) during 1982-2011 are 0.87 ($p < 0.01$) and 14 mm/year respectively. This
290 suggests the good performance of the CSSPv2 in simulating the hydrological
291 processes over the Sanjiangyuan region. Although meteorological and ecological
292 outputs from CMIP6 models have coarse resolutions (~100 km), the land surface
293 simulation driven by bias corrected CMIP6 results (CMIP6_His/CSSPv2) also
294 captures the terrestrial hydrological variations reasonably well. The Kling-Gupta
295 efficiency of the ensemble mean streamflow simulation reaches up to 0.71~0.81, and
296 the ensemble mean monthly Terrestrial Water Storage Anomaly (TWSA) and annual
297 evapotranspiration generally agree with observations and other reference data
298 (Figures 3c-3d).

299 Figure 4 shows relative changes of terrestrial hydrological variables over the
300 Sanjiangyuan region at different warming levels. The ensemble mean of the increase
301 in annual precipitation is 5% at 1.5°C warming level, and additional 0.5°C and 1.5°C
302 warming will further increase the wetting trends to 7% and 13% respectively. Annual
303 evapotranspiration experiences significant increases at all warming levels, and the
304 ensemble mean increases are 4%, 7% and 13% at 1.5, 2.0 and 3.0°C warming levels
305 respectively. The ratio of transpiration to evapotranspiration also increases
306 significantly, indicating that vegetation transpiration increases much larger than the
307 soil evaporation and canopy evaporation. Although annual total runoff has larger
308 relative changes than evapotranspiration (6%, 9% and 14% at 1.5, 2.0 and 3.0°C
309 warming levels respectively), the uncertainty is large as only 75% of the models show
310 positive signals, which may be caused by large uncertainty in the changes during
311 summer and autumn seasons. The terrestrial water storage (TWS) which includes
312 foliage water, surface water, soil moisture and groundwater, shows slightly decreasing
313 trend at annual scale, suggesting that the increasing precipitation in the future
314 becomes extra evapotranspiration and runoff instead of recharging the local water
315 storage. The accelerated terrestrial hydrological cycle also exists at seasonal scale, as
316 the seasonal changes are consistent with the annual ones.

317 **3.2 Changes in streamflow extremes at different warming levels**

318 Although the intensified terrestrial hydrology induces more streamflow over the
319 headwater region of Yellow river during winter and spring months, streamflow does
320 not increase and even decreases during the flood season (July-September; Figure 5a).

321 Figure 5b shows the changes of streamflow dry extremes over the Yellow river source
322 region at different warming levels, with the error bars showing estimated uncertainties.
323 The frequency of streamflow dry extremes over the Yellow river is found to increase
324 by 55% at 1.5°C warming level (Figure 5b), but the uncertainty is larger than the
325 ensemble mean. However, the dry extreme frequency will further increase to 77% and
326 125% at the 2.0 and 3.0°C warming levels and the results become significant (Figure
327 5b). No statistically significant changes are found for the wet extremes at all warming
328 levels over the Yellow River headwater region, as the uncertainty ranges are larger
329 than the ensemble means.

330 Over the Yangtze river headwater region, streamflow increases in all months at
331 different warming levels (Figure 5c). The frequency of wet extremes increases
332 significantly by 138%, 202% and 232% at 1.5, 2.0 and 3.0°C warming levels (Figure
333 5d), suggesting a higher risk of flooding. Although the frequency of dry extremes also
334 tends to decrease significantly by 35%, 44%, 34% at the three warming levels, the
335 changes are much smaller than those of the wet extremes. Moreover, contributions
336 from climate change and ecological change are both smaller than the uncertainty
337 ranges (not shown), suggesting that their impacts on the changes of dry extremes over
338 the Yangtze river headwater region are not distinguishable. Thus, we mainly focus on
339 the dry extremes over the Yellow river and the wet extremes over the Yangtze river in
340 the following analysis.

341 Different changes of streamflow extremes over the Yellow and Yangtze rivers
342 can be interpreted from different accelerating rates of precipitation and

343 evapotranspiration. Figure 6 shows probability density functions (PDFs) of
344 precipitation, evapotranspiration and their difference (P-ET, i.e. residual water for
345 runoff generation) during the flood season. Over the Yellow river, PDFs of
346 precipitation and evapotranspiration both shift to the right against the reference period,
347 except for the precipitation at 1.5°C warming level. However, the increasing trend of
348 evapotranspiration is stronger than that of precipitation, leading to a left shift ~~of~~ for the
349 PDF ~~of~~ P-ET. Moreover, increased variations of precipitation and
350 evapotranspiration, as indicated by the increased spread of their PDFs, also lead to a
351 larger spread of PDFs of P-ET. The above two factors together induce a heavier left
352 tail in the PDF of P-ET for the warming future than the reference period (Figure 6e).
353 The probability of P-ET<80mm increases from 0.1 during historical period to 0.11,
354 0.13 and 0.16 at 1.5, 2.0 and 3.0°C warming levels individually. This indicates a
355 higher probability of less water left for runoff generation at different warming levels,
356 given little changes in TWS (section 3.1). Moreover, Figure 6e also shows little
357 change ~~to~~ in the right tails ~~in~~ of the PDF of P-ET as probability for P-ET>130mm stays
358 around 0.1 at different warming levels, suggesting little change to the probability of
359 high residual water. This is consistent with the insignificant wet extreme change over
360 the Yellow river. Over the Yangtze river, however, intensified precipitation is much
361 larger than the increased evapotranspiration, leading to a systematic rightward shift of
362 the PDF of P-ET (Figures 6b, 6d and 6f). Thus both the dry and wet extremes show
363 significant changes over the Yangtze river.

364 **3.3 Influences of land cover change and CO₂ physiological forcing**

365 Figures 7a-7b show the changes of streamflow extremes (compared with the
366 reference period) induced by climate and ecological factors. Although the contribution
367 from climate change (red bars in Figures 7a-7b) is greater than the ecological factors
368 (blue and cyan bars in in Figures 7a-7b), influences of CO₂ physiological forcing and
369 land cover change are nontrivial. The CO₂ physiological forcing tends to alleviate dry
370 extremes (or increase wet extremes), while land cover change plays a contrary role.
371 Over the Yellow river, the combined impact of the two ecological factors (sum of blue
372 and cyan bars) reduces the increasing trend of dry extremes caused by climate change
373 (red bars) by 18~22% at 1.5 and 2.0 °C warming levels, while intensifies the dry
374 extremes by 9% at 3.0°C warming level. This can be interpreted from their
375 contributions to the evapotranspiration, as ~~the increased LAI~~ enhancement [effect of](#)
376 [the increased LAI](#) on ET is weaker than the suppression effect of CO₂ physiological
377 [impactforcing](#) at 1.5 and 2.0°C warming levels, while stronger at 3.0°C warming level
378 (not shown). Over the Yangtze river, similarly, combined effect of land cover and CO₂
379 physiological forcing increases the wet extremes by 9% at 1.5°C warming level while
380 decreases the wet extremes by 12% at 3.0°C warming level.

381 In addition, Figures 7c and 7d show that the combined impact of CO₂
382 physiological forcing and land cover change also influences the differences between
383 different warming levels. Over the Yellow river, climate change increases dry
384 extremes by 26% from 1.5 to 2.0°C warming level, and by 40% from 1.5 and 3.0°C
385 warming level (red bars in Figure 7c). After considering the two ecological factors
386 (pink bars in Figure 7c), above two values change to 22% and 70% respectively, and

387 the difference between 1.5 and 3.0°C warming levels becomes significant. For the wet
388 extreme over the Yangtze river (Figure 7d), the climate change induced difference
389 between 1.5 and 2.0°C warming levels is decreased by 16% after accounting for the
390 two ecological factors. And this decrease reaches up to 49% for the difference
391 between 1.5 and 3.0°C warming levels. We also compared the scenarios when CO₂
392 physiological forcing and land cover change are combined with climate change
393 individually (blue and cyan bars in Figures 7c-d), and the results show the land cover
394 change dominates their combined influences on the difference between different
395 warming levels.

396 **4 Conclusions and Discussion**

397 This study investigates changes of streamflow extremes over the Sanjiangyuan
398 region at different global warming levels through high-resolution land surface
399 modeling driven by CMIP6 climate simulations. The terrestrial hydrological cycle
400 under global warming of 1.5°C is found to accelerate by 4~6% compared with the
401 reference period of 1985-2014, according to the relative changes of precipitation,
402 evapotranspiration and total runoff. The terrestrial water storage, however, shows a
403 slight but significant decreasing trend as increased evapotranspiration and runoff are
404 larger than the increased precipitation. This decreasing trend of terrestrial water
405 storage in the warming future is also found in six major basins in China (Jia et al.,
406 2020). Although streamflow changes during the flood season has a large uncertainty,
407 the frequency of wet extremes over the Yangtze river will increase significantly by
408 138% and that of dry extremes over the Yellow river will increase by 55% compared

409 with that during 1985~2014. With an additional 0.5°C warming, the frequency of dry
410 and wet extremes will increase further by 22~64%. If the global warming is not
411 adequately managed (e.g., to reach 3.0°C), wet extremes over the Yangtze river and
412 dry extremes over the Yellow river will increase by 232% and 125%. The changes
413 from 1.5 to 2.0 and 3.0°C are nonlinear compared with that from reference period to
414 1.5°C, which are also found for some fixed-threshold climate indices over the Europe
415 (Dosio and Fischer, 2018). It is necessary to cap the global warming at 2°C or even
416 lower level, to reduce the risk of wet and dry extremes over the Yangtze and Yellow
417 rivers.

418 This study also shows the nontrivial contributions from land cover change and
419 CO₂ physiological forcing to the extreme streamflow changes especially at 2.0 and
420 3.0°C warming levels. The CO₂ physiological forcing is found to increase streamflow
421 and reduce the dry extreme frequency by 14~24%, which is consistent with previous
422 [research findings](#) that CO₂ physiological forcing would increase available water and
423 reduce water stress at the end of this century (Wiltshire et al., 2013). However, our
424 results further show that the drying effect of increasing LAI on streamflow will
425 exceed the wetting effect of CO₂ physiological forcing at 3.0°C warming level (during
426 2048~2075) over the Sanjiangyuan region, making a reversion in the combined
427 impacts of CO₂ physiological forcing and land cover. Thus it is vital to consider the
428 impact of land cover change in the projection of future water stress especially at high
429 warming scenarios.

430 Moreover, about 43~52% of the extreme streamflow changes between 1.5 and

431 3.0°C warming levels are attributed to the increased LAI. Considering the LAI
432 projections from different CMIP6 models are induced by the climate change, it can be
433 inferred that the indirect influence of climate change (e.g., through land cover change)
434 has the same and even larger importance on the changes of streamflow extremes
435 between 1.5 and 3.0°C or even higher warming levels, compared with the direct
436 influence (e.g., through precipitation and evapotranspiration). Thus, it is vital to
437 investigate hydrological and its extremes changes among different warming levels
438 from an eco-hydrological perspective instead of focusing on climate change alone.

439 Although we used 11 CMIP6 models combined with two SSP scenarios to reduce
440 the uncertainty of future projections caused by GCMs, using a single land surface
441 model may result in uncertainties (Marx et al., 2018). However, considering the good
442 performance of the CSSPv2 land surface model over the Sanjiangyuan region and the
443 dominant role of GCMs' uncertainty (Zhao et al., 2019; Samaniego et al., 2017),
444 uncertainty from the CSSPv2 model should have limited influence on the robustness
445 of the result.

446

447 **Acknowledgments** We thank the World Climate Research Programme's Working
448 Group on Coupled modelling for providing CMIP6 data (<https://esgf-node.llnl.gov>).
449 This work was supported by National Key R&D Program of China
450 (2018YFA0606002) and National Natural Science Foundation of China (41875105,
451 91547103), and the Startup Foundation for Introducing Talent of NUIST.

452

453 **Competing interests**

454 The authors declare that they have no conflict of interest.

455

456 **References**

- 457 Bibi, S., Wang, L., Li, X., Zhou, J., Chen, D., and Yao, T.: Climatic and associated
458 cryospheric, biospheric, and hydrological changes on the Tibetan Plateau: a
459 review, *Int. J. Climatol.*, 38, e1-e17, <https://doi.org/10.1002/joc.5411>, 2018.
- 460 Chen, J., Gao, C., Zeng, X., Xiong, M., Wang, Y., Jing, C. Krysanova, V., Huang, J.,
461 Zhao, N., and Su, B.: Assessing changes of river discharge under global warming
462 of 1.5 ° C and 2 ° C in the upper reaches of the Yangtze River Basin: Approach
463 by using multiple-GCMs and hydrological models, *Quatern. Int.*, 453, 1 - 11,
464 <http://dx.doi.org/10.1016/j.quaint.2017.01.017>, 2017.
- 465 Cuo, L., Zhang, Y., Zhu, F., and Liang, L.: Characteristics and changes of streamflow
466 on the Tibetan Plateau: A review, *J. Hydrol.-Reg. Stud.*, 2, 49 - 68,
467 <https://doi.org/10.1016/j.ejrh.2014.08.004>, 2014.
- 468 Dai, Y. J., Zeng, X. B., Dickinson, R. E., Baker, I., Bonan, G. B., Bosilovich, M. G.,
469 Denning, A. S., Dirmeyer, P. A., Houser, P. R., Niu, G. Y., Oleson, K. W.,
470 Schlosser, C. A., and Yang, Z. L.: The Common Land Model. *B. Am. Meteorol.*
471 *Soc.*, 84, 1013 - 1024, <https://doi.org/10.1175/BAMS-84-8-1013>, 2003.
- 472 Döll, P., Trautmann, T., Gerten, D., Schmied, H. M., Ostberg, S., Saaed, F., and
473 Schleussner, C.: Risks for the global freshwater system at 1.5 ° C and 2 ° C
474 global warming. *Environ. Res. Lett.*, 13, 044038,
475 <https://doi.org/10.1088/1748-9326/aab792>, 2018.
- 476 Dosio, A., and Fischer, E. M.: Will half a degree make a difference? Robust
477 projections of indices of mean and extreme climate in Europe under 1.5 ° C, 2 °

478 C, and 3 ° C global warming, *Geophys. Res. Lett.*, 45.
479 <https://doi.org/10.1002/2017GL076222>, 2018.

480 Eyring, V., Bony, S., Meehl, G. A., Senior, C. A., Stevens, B., Stouffer, R. J., and
481 Taylor, K. E.: Overview of the Coupled Model Intercomparison Project Phase 6
482 (CMIP6) experimental design and organization, *Geosci. Model Dev.*, 9, 1937 –
483 1958. <https://doi.org/10.5194/gmd-9-1937-2016>, 2016.

484 Fowler, M. D., Kooperman G. J., Randerson, J. T. and Pritchard M. S.: The effect of
485 plant physiological responses to rising CO₂ on global streamflow, *Nat. Clim.*
486 *Change*, 9, 873-879, <https://doi.org/10.1038/s41558-019-0602-x>, 2019.

487 He, J., Yang, K., Tang, W., Lu, H., Qin, J., Chen, Y., and Li, X.: The first
488 high-resolution meteorological forcing dataset for land process studies over
489 China, *Sci. Data*, 7, 25. <https://doi.org/10.1038/s41597-020-0369-y>, 2020.

490 Hempel, S., Frieler, K., Warszawski, L., and Piontek, F.: A trend-preserving bias
491 correction-the ISI-MIP approach, *Earth Syst. Dyn.*, 4, 219-236.
492 <https://doi.org/10.5194/esd-4-219-2013>, 2013.

493 [Hoegh-Guldberg, O., Jacob, D., Taylor, M., Bindi, M., Brown, S., Camilloni, I.,](#)
494 [Diedhiou, A., Djalante, R., Ebi, K. L., Engelbrecht, F., Guiot, J., Hijjoka, Y.,](#)
495 [Mehrotra, S., Payne, A., Seneviratne, S. I., Thomas, A., Warren, R., and Zhou,](#)
496 [G.:](#) [Impacts of 1.5 ° C Global Warming on Natural and Human Systems, in:](#)
497 [Global Warming of 1.5°C. An IPCC Special Report on the impacts of global](#)
498 [warming of 1.5°C above pre-industrial levels and related global greenhouse gas](#)
499 [emission pathways, in the context of strengthening the global response to the](#)

500 [threat of climate change, sustainable development, and efforts to eradicate](#)
501 [poverty, edited by: MassonDelmotte,V., Zhai, P., Pörtner, H.-O., Roberts, D.,](#)
502 [Skea, J., Shukla, P.R., Pirani, A., Moufouma-Okia, W., Péan, C., Pidcock, R.,](#)
503 [Connors, S., Matthews, J.B.R., Chen, Y., Zhou, X., Gomis, M.I., Lonnoy, E.,](#)
504 [Maycock, T., Tignor M., and Waterfield, T.\]. In Press, 186-203,](#)
505 <https://www.ipcc.ch/sr15/>, 2018.

506 Ji, P., and Yuan, X.: High-resolution land surface modeling of hydrological changes
507 over the Sanjiangyuan region in the eastern Tibetan Plateau: 2. Impact of climate
508 and land cover change, *J. Adv. Model. Earth. Sy.*, 10, 2829 – 2843.
509 <https://doi.org/10.1029/2018MS001413>, 2018.

510 Jia, B., Cai, X., Zhao, F., Liu, J., Chen, S., Luo, X., Xie, Z., and Xu, J.: Potential
511 future changes of terrestrial water storage based on climate projections by
512 ensemble model simulations, *Adv. Water Resour.*, 142, 103635.
513 <https://doi.org/10.1016/j.advwatres.2020.103635>, 2020.

514 Jung, M., Reichstein, M., and Bondeau, A.: Towards global empirical upscaling of
515 FLUXNET eddy covariance observations: Validation of a model tree ensemble
516 approach using a biosphere model, *Biogeosciences*, 6, 2001–2013.
517 <https://doi.org/10.5194/bg-6-2001-2009>, 2009.

518 Kuang, X., and Jiao, J.: Review on climate change on the Tibetan Plateau during the
519 last half century, *J. Geophys. Res. Atmos.*, 121, 3979 – 4007.
520 <https://doi.org/10.1002/2015JD024728>, 2016.

521 Li, J., Liu, D., Li, Y., Wang, S., Yang, Y., Wang, X., Guo, H., Peng, S., Ding, J., Shen,
522 M., and Wang, L.: Grassland restoration reduces water yield in the headstream
523 region of Yangtze River, *Sci. Rep.*, 7, 2162,
524 <https://doi.org/10.1038/s41598-017-02413-9>, 2017.

525 Li, W., Jiang, Z., Zhang, X., Li, L. and Sun, Y.: Additional risk in extreme
526 precipitation in China from 1.5 ° C to 2.0 ° C global warming levels, *Sci.*
527 *Bull.*, 63, 228. <https://doi.org/10.1016/j.scib.2017.12.021>, 2018.

528 Liang, L., Li, L., Liu, C., and Cuo, L.: Climate change in the Tibetan Plateau Three
529 Rivers Source Region: 1960 – 2009, *Int. J. Climatol.*, 33, 2900-2916.
530 <https://doi.org/10.1002/joc.3642>, 2013.

531 Liang, X., Lettenmaier, D. P., Wood, E. F., and Burges, S. J.: A simple hydrologically
532 based model of land surface water and energy fluxes for general circulation
533 models, *J. Geophys. Res.*, 99, 14,415-14,428. <https://doi.org/10.1029/94JD00483>,
534 1994.

535 Marcott, S. A., Shakun, J. D., Clark, P. U., and Mix, A. C.: A Reconstruction of
536 Regional and Global Temperature for the Past 11,300 Years, *Science*, 339, 1198
537 – 1201. <https://doi.org/10.1126/science.1228026>, 2013.

538 Martens, B., Miralles, D. G., Lievens, H., van der Schalie, R., de Jeu, R. A. M.,
539 Fernández-Prieto, D., Beck, H. E., Dorigo, W. A., and Verhoest, N. E. C.:
540 GLEAM v3: satellite-based land evaporation and root-zone soil moisture, *Geosci.*
541 *Model Dev.*, 10, 1903–1925. <https://doi.org/10.5194/gmd-10-1903-2017>, 2017.

542 Marx, A., Kumar, R., and Thober, S.: Climate change alters low flows in Europe
543 under global warming of 1.5, 2, and 3 ° C, *Hydrol. Earth. Syst. Sc.*, 22, 1017 –
544 1032. <https://doi.org/10.5194/hess-22-1017-2018>, 2018.

545 Meinshausen, M., Nicholls, Z. R. J., Lewis, J., Gidden, M. J., Vogel, E., Freund, M.,
546 Beyerle, U., Gessner, C., Nauels, A., Bauer, N., Canadell, J. G., Daniel, J. S.,
547 John, A., Krummel, P. B., Luderer, G., Meinshausen, N., Montzka, S. A., Rayner,
548 P. J., Reimann, S., Smith, S. J., van den Berg, M., Velders, G. J. M., Vollmer, M.
549 K., and Wang, R. H. J.: The shared socio-economic pathway (SSP) greenhouse
550 gas concentrations and their extensions to 2500, *Geosci. Model Dev.*, 13, 3571 –
551 3605, <https://doi.org/10.5194/gmd-13-3571-2020>, 2020.

552 Meinshausen, M., Vogel, E., and Nauels, A., Lorbacher, K., Meinshausen, N.,
553 Etheridge, D. M., Fraser, P. J., Montzka, S. A., Rayner, P. J., Trudinger, C. M.,
554 Krummel, P. B., Beyerle, U., Canadell, J. G., Daniel, J. S., Enting, I. G., Law, R.
555 M., Lunder, C. R., O'Doherty, S., Prinn, R. G., Reimann, S., Rubino, M., Velders,
556 G. J. M., Vollmer, M. K., Wang, R. H. J., and Weiss, R.: Historical greenhouse
557 gas concentrations for climate modelling (CMIP6), *Geosci. Model Dev.*, 10,
558 2057-2116. <https://doi.org/10.5194/gmd-10-2057-2017>, 2017.

559 Mohammed, K., Islam, A. S., Islam, G. M. T., Alfieri, L., Bala, S. K., and Khan, M. J.
560 U.: Extreme flows and water availability of the Brahmaputra River under 1.5 and
561 2 ° C global warming scenarios, *Climatic Change*, 145, 159-175.
562 <https://doi.org/10.1007/s10584-017-2073-2>, 2017.

563 Morice, C. P., Kennedy J. J., Rayner N. A., and Jones P. D.: Quantifying uncertainties
564 in global and regional temperature change using an ensemble of observational
565 estimates: The HadCRUT4 dataset, *J. Geophys. Res.*, 117, D08101.
566 <https://doi.org/10.1029/2011JD017187>, 2012.

567 Oleson, K. W., Lawrence, D. M., Bonan, G. B., Drewniak, B., Huang, M., Koven, C.
568 D., Levis, S., Li, F., Riley, W. J., Subin, Z. M., Swenson, S. C., Thornton, P. E.,
569 Bozbiyik, A., Fisher, R., Heald, C. L., Kluzek, E., Lamarque, J. F., Lawrence, P.
570 J., Leung, L. R., Lipscomb, W., Muszala, S., Ricciuto, D. M., Sacks, W., Sun, Y.,
571 Tang, J., Yang, Z. L.: Technical description of version 4.5 of the Community
572 Land Model (CLM) (Rep. NCAR/TN-503 + STR, 420), 2013.

573 O'Neill, B. C., Tebaldi, C., Vuuren, D. P. V., Eyring, V., Friedlingstein, P., Hurtt, G.,
574 Knutti, R., Kriegler, E., Lamarque, J. F., Lowe, J., Meehl, G. A., Moss, R., Riahi,
575 K., and Sanderson, B. M.: The scenario model intercomparison project
576 (ScenarioMIP) for CMIP6, *Geosci. Model Dev.*, 9, 3461-3482.
577 <https://doi.org/10.5194/gmd-9-3461-2016>, 2016.

578 Samaniego, L., Kumar, R., Breuer, L., Chamorro, A., Flörke, M., Pechlivanidis, I. G.,
579 Schäfer, D., Shah, H., Vetter, T., Wortmann, M., and Zeng, X.: Propagation of
580 forcing and model uncertainties on to hydrological drought characteristics in a
581 multi-model century-long experiment in large river basins, *Climatic Change*, 141,
582 435-449. <https://doi.org/10.1007/s10584-016-1778-y>, 2017.

583 Thober, T., Kumar, R., and Waders, N.: Multi-model ensemble projections of
584 European river floods and high flows at 1.5, 2, and 3 degrees global warming,

585 Environ. Res. Lett., 13, 014003. <https://doi.org/10.1088/1748-9326/aa9e35>,
586 2018.

587 Vicente-Serrano, S. M., Lopez-Moreno, J. I., Begueria, S., Lorenzo-Lacruz, J.,
588 Azorin-Molina, C., and Moran-Tejeda, E.: Accurate computation of a streamflow
589 drought index, J. Hydrol. Eng., 17, 318 – 332.
590 [https://doi.org/10.1061/\(Asce\)He.1943-5584.0000433](https://doi.org/10.1061/(Asce)He.1943-5584.0000433), 2012.

591 Watkins, M. M., Wiese, D. N., Yuan, D. N., Boening, C., and Landerer, F. W.:
592 Improved methods for observing Earth’s time variable mass distribution with
593 GRACE using spherical cap mascons, J. Geophys. Res. Solid Earth, 120,
594 2648-2671. <https://doi.org/10.1002/2014JB011547>, 2015.

595 Wiltshire, A., Gornall, J., Booth, B., Dennis, E., Falloon, P., Kay, G., McNeill, D.,
596 McSweeney, C. and Betts, R.: The importance of population, climate change and
597 CO2 plant physiological forcing in determining future global water stress, Global
598 Environ. Change, 23(5), 1083-1097.
599 <http://dx.doi.org/10.1016/j.gloenvcha.2013.06.005>, 2013.

600 WMO.: WMO Statement on the State of the Global Climate in 2019,
601 https://library.wmo.int/doc_num.php?explnum_id=10211, 2020.

602 [Xu, R., Hu, H., Tian, F., Li, C., and Khan, M. Y. A.: Projected climate change impacts](#)
603 [on future streamflow of the Yarlung Tsangpo-Brahmaputra River, Global Planet.](#)
604 [Change, 175: 144-159. https://doi.org/10.1016/j.gloplacha.2019.01.012, 2019.](#)

605 Yang, K., Wu, H., Qin, J., Lin, C., Tang, W., and Chen, Y.: Recent climate changes
606 over the Tibetan plateau and their impacts on energy and water cycle: A review,

607 Global Planet. Change, 112, 79 – 91.
608 <https://doi.org/10.1016/j.gloplacha.2013.12.001>, 2013.

609 Yang, Y., Rodericj, M. L., Zhang, S., McVicar, T. R., and Donohue, R. J.: Hydrologic
610 implications of vegetation response to elevated CO2 in climate projections, Nat.
611 Clim. Change, 9, 44-48. <https://doi.org/10.1038/s41558-018-0361-0>, 2019.

612 Yuan, X., Ji, P., Wang, L., Liang, X., Yang, K., Ye, A., Su, Z., and Wen, J.: High
613 resolution land surface modeling of hydrological changes over the Sanjiangyuan
614 region in the eastern Tibetan Plateau: 1. Model development and evaluation, J.
615 Adv. Model. Earth. Sy., 10, 2806 – 2828. <https://doi.org/10.1029/2018MS001413>,
616 2018a.

617 Yuan, X., Jiao, Y., Yang, D., and Lei, H.: Reconciling the attribution of changes in
618 streamflow extremes from a hydroclimate perspective, Water Resour. Res., 54,
619 3886 – 3895. <https://doi.org/10.1029/2018WR022714>, 2018b.

620 Yuan, X., Zhang, M., Wang, L., and Zhou, T.: Understanding and seasonal forecasting
621 of hydrological drought in the Anthropocene, Hydrol. Earth. Syst. Sc., 21, 5477
622 – 5492. <https://doi.org/10.5194/hess-21-5477-2017>, 2017.

623 Zhang Y., You Q., Chen C., and Ge J.: Impacts of climate change on streamflows
624 under RCP scenarios: A case study in Xin River Basin, China, Atmos. Res.,
625 178-179, 521-534. <http://dx.doi.org/10.1016/j.atmosres.2016.04.018>, 2016.

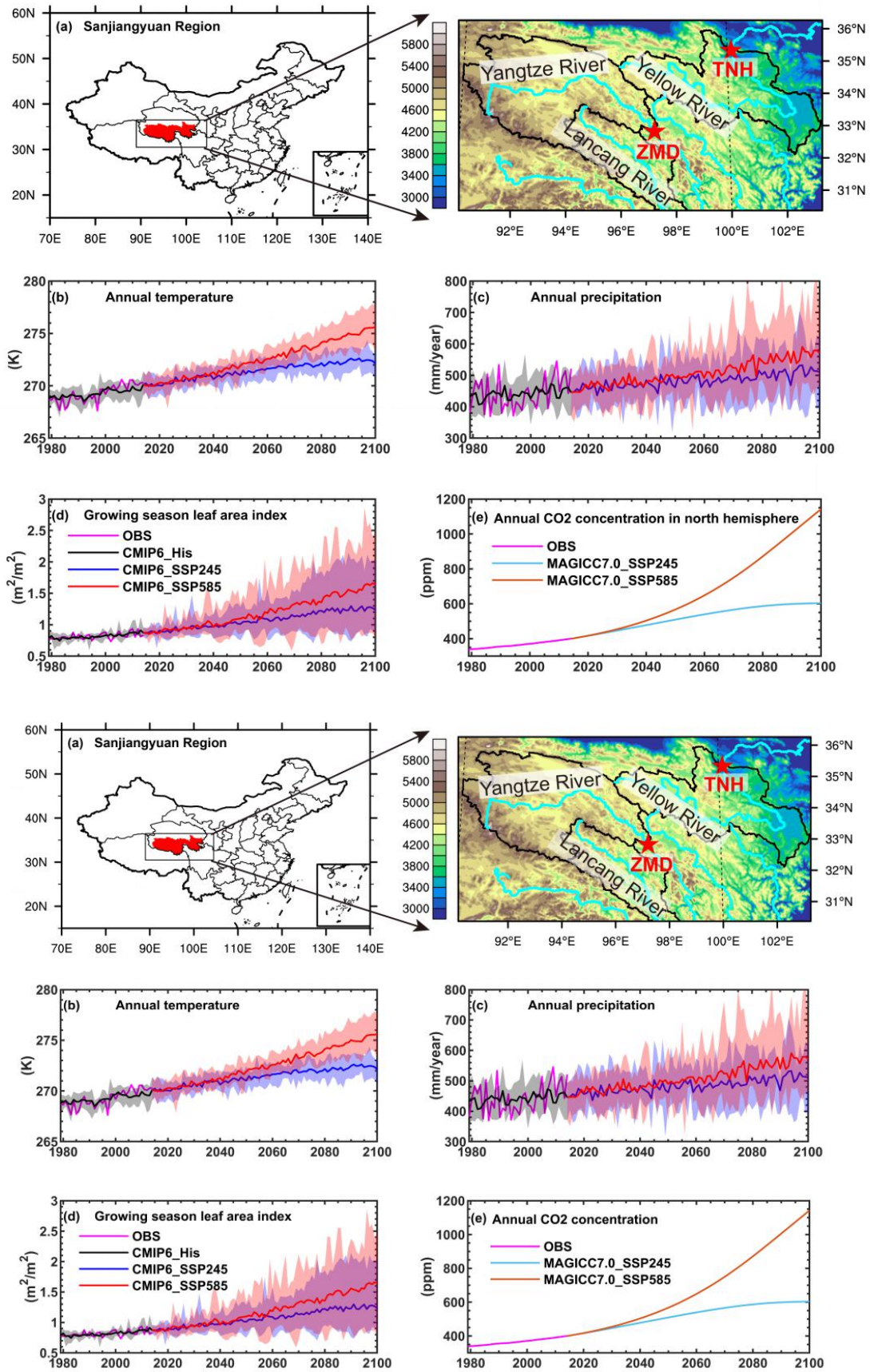
626 Zhao Q., Ding Y., Wang J., Gao H., Zhang S., Zhao C. Xu J. Han H., and Shanguan
627 D.: Projecting climate change impacts on hydrological processes on the Tibetan
628 Plateau with model calibration against the glacier inventory data and observed

629 streamflow, *J. Hydrol.*, 573, 60-81. <https://doi.org/10.1016/j.jhydrol.2019.03.043>,
630 2019.

631 Zhu Q., Jiang H., Peng C., Liu J., Fang X., Wei X., Liu S., and Zhou G.: Effects of
632 future climate change, CO₂ enrichment, and vegetation structure variation on
633 hydrological processes in China, *Global Planet. Change*, 80-81, 123-135.
634 <https://doi.org/10.1016/j.gloplacha.2011.10.010>, 2012.

635 Zhu, Z. C., Piao, S. L., Myneni, R. B., Huang, M. T., Zeng, Z. Z., Canadell, J. G.,
636 Ciais, P., Sitch, S., Friedlingstein, P., Arneeth, A., Cao, C. X., Cheng, L., Kato, E.,
637 Koven, C., Li, Y., Lian, X., Liu, Y. W., Liu, R. G., Mao, J. F., Pan, Y. Z., Peng, S.
638 S., Penuelas, J., Poulter, B., Pugh, T. A. M., Stocker, B. D., Viovy, N., Wang, X.
639 H., Wang, Y. P., Xiao, Z. Q., Yang, H., Zaehle, S., and Zeng, N.: Greening of the
640 Earth and its drivers, *Nature Climate Change*, 6(8), 791-+,
641 <https://doi.org/10.1038/Nclimate3004>, 2016.

642



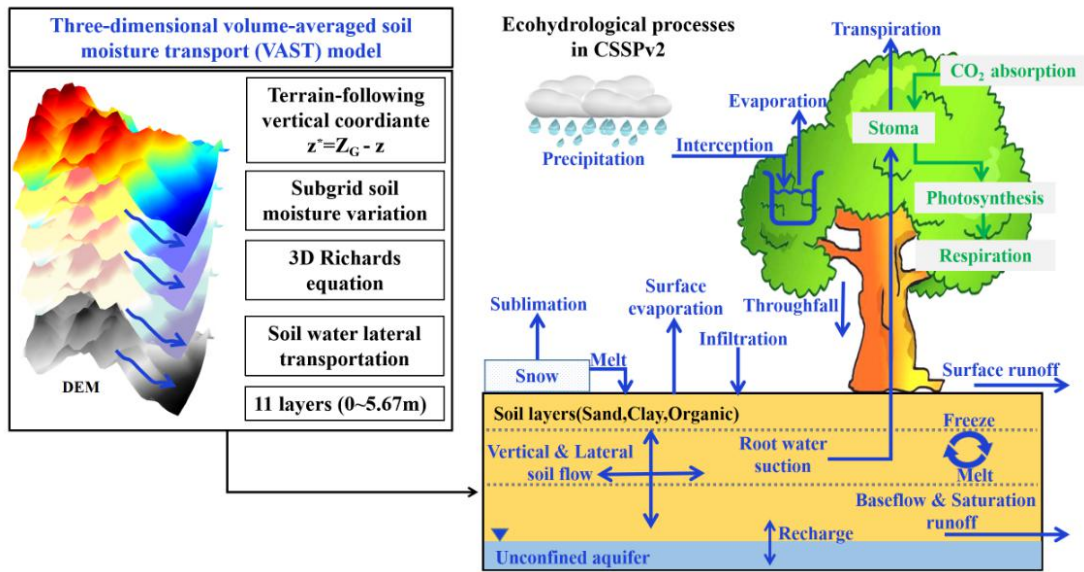
643

644

645 **Figure 1.** (a) The locations of the Sanjiangyuan region and streamflow gauges.

646 (b)-(ed) are †The time series of annual temperature, precipitation, and growing season
647 leaf area index and CO₂ concentration averaged over the Sanjiangyuan region during
648 1979-2100. (e) Observed and simulated annual CO₂ concentration over the
649 Sanjiangyuan region. Red pentagrams in (a) are two streamflow stations named
650 Tangnaihai (TNH) and Zhimenda (ZMD). Black, blue and red lines in (b-d) are
651 ensemble means of CMIP6 model simulations from the historical, SSP245 and
652 SSP585 experiments. Shadings are ranges of individual ensemble members. Cyan and
653 brown lines in (e) are future CO₂ concentration under SSP245 and SSP585 scenarios
654 simulated by MAGICC7.0 model.
655

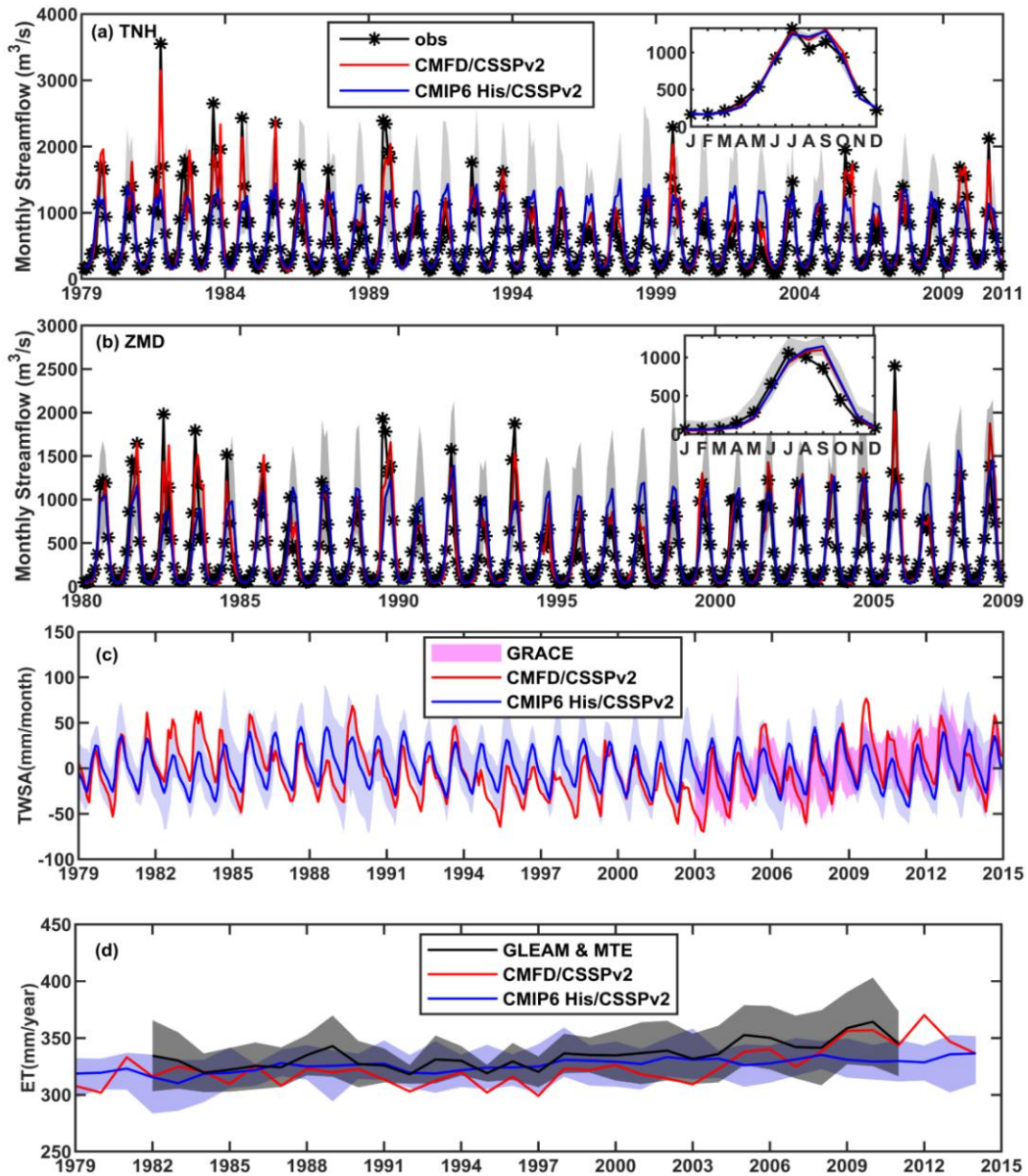
656



657

658 **Figure 2.** Main ecohydrological processes in the Conjunctive Surface-Subsurface

659 Process version 2 (CSSPv2) land surface model.



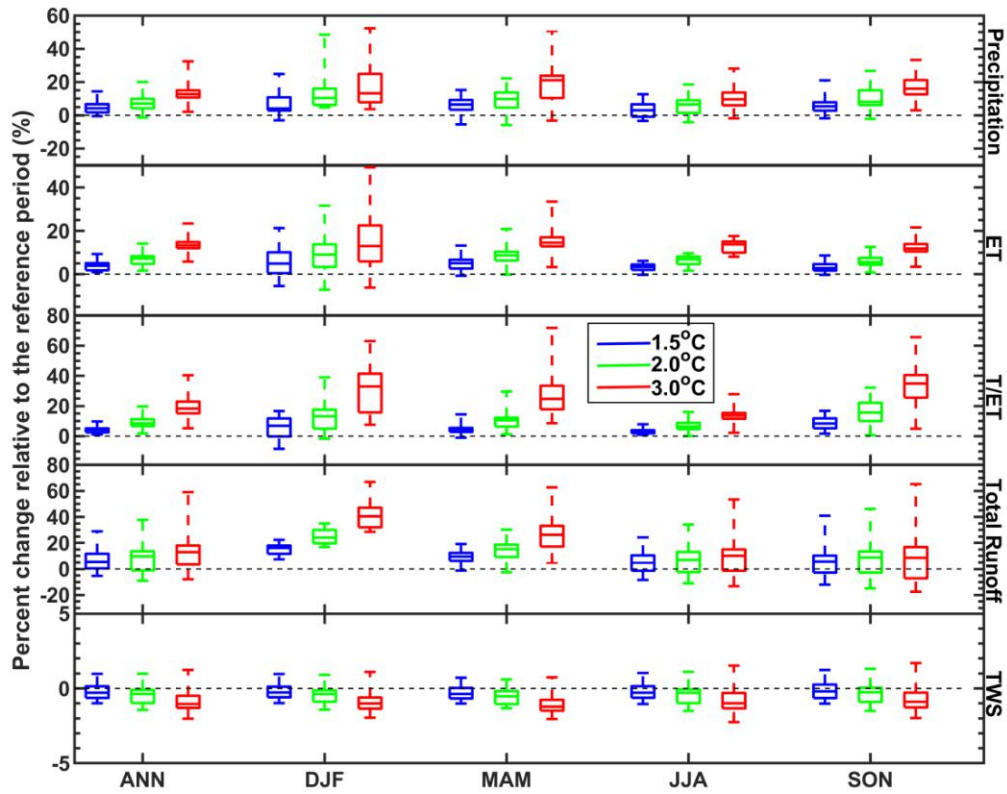
660

661 **Figure 3.** Evaluation of model simulations. (a-b) Observed and simulated monthly
 662 streamflow at the Tangnaihai (TNH) and Zhimenda (ZMD) hydrological stations, with
 663 the climatology shown in the upper-right corner. (c-d) Evaluation of the simulated
 664 monthly terrestrial water storage anomaly (TWSA) and annual evapotranspiration (ET)
 665 averaged over the Sanjiangyuan region. Red lines are CSSPv2 simulation forced by
 666 observed meteorological forcing. Blue lines represent ensemble means of 11
 667 CMIP6_His/CSSPv2 simulations, while gray shadings in (a-b) and blue shadings in
 668 (c-d) are ranges of individual ensemble members. Pink shading in (c) is GRACE

669 satellite observations. Black line and black shading in (d) are ensemble mean and
670 ranges of GLEAM_ET and MTE_ET datasets.

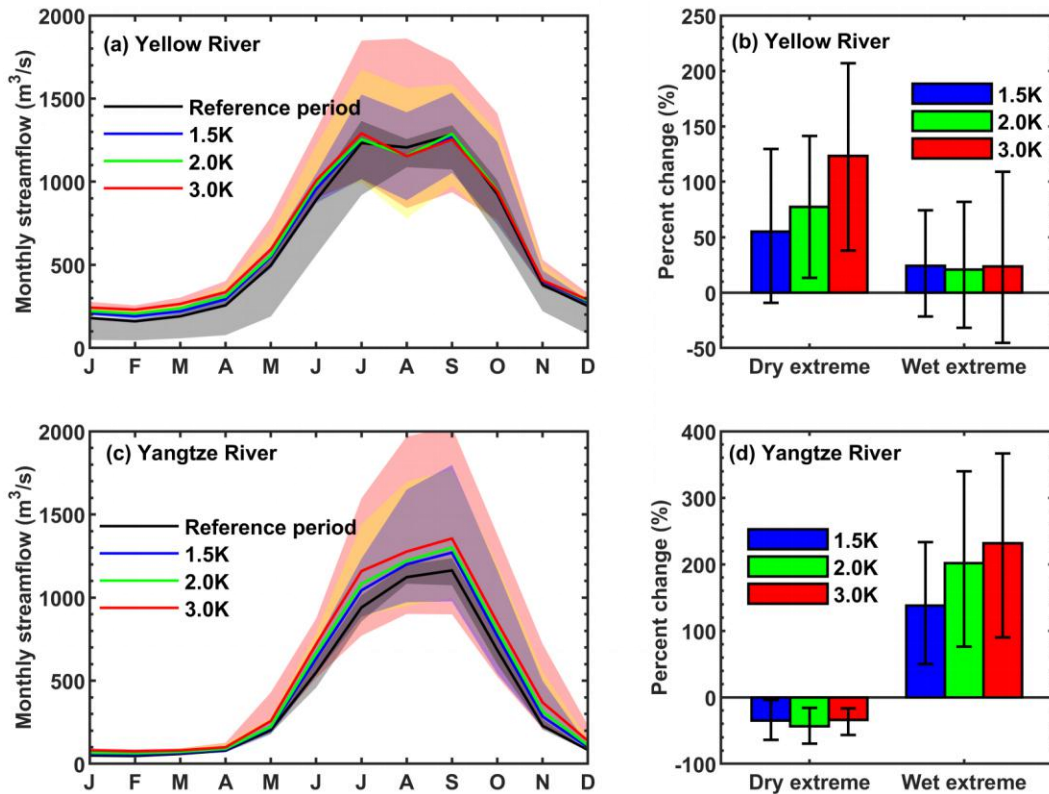
671

672



673

674 **Figure 4.** Box plots of relative changes of regional mean precipitation,
 675 evapotranspiration (ET), ratio of transpiration to evapotranspiration (T/ET), total
 676 runoff and terrestrial water storage (TWS) at different global warming levels.
 677 Reference period is 1985-2014, and annual (ANN) and seasonal (winter: DF, spring:
 678 MAM, summer: JJA and autumn: SON) results are all shown. Boxes show 25th to
 679 75th ranges among 22 CMIP6_SSP/CSSPv2 simulations, while lines in the boxes are
 680 median values.



682

683 **Figure 5.** Changes of streamflow and its extremes at the outlets of the headwater

684 regions of the Yellow river and the Yangtze river, i.e., Tangnaihai gauge and

685 Zhimenda gauge. (a) Simulated monthly streamflow over the Yellow river during the

686 reference period (1985-2014) and the periods with different global warming levels.

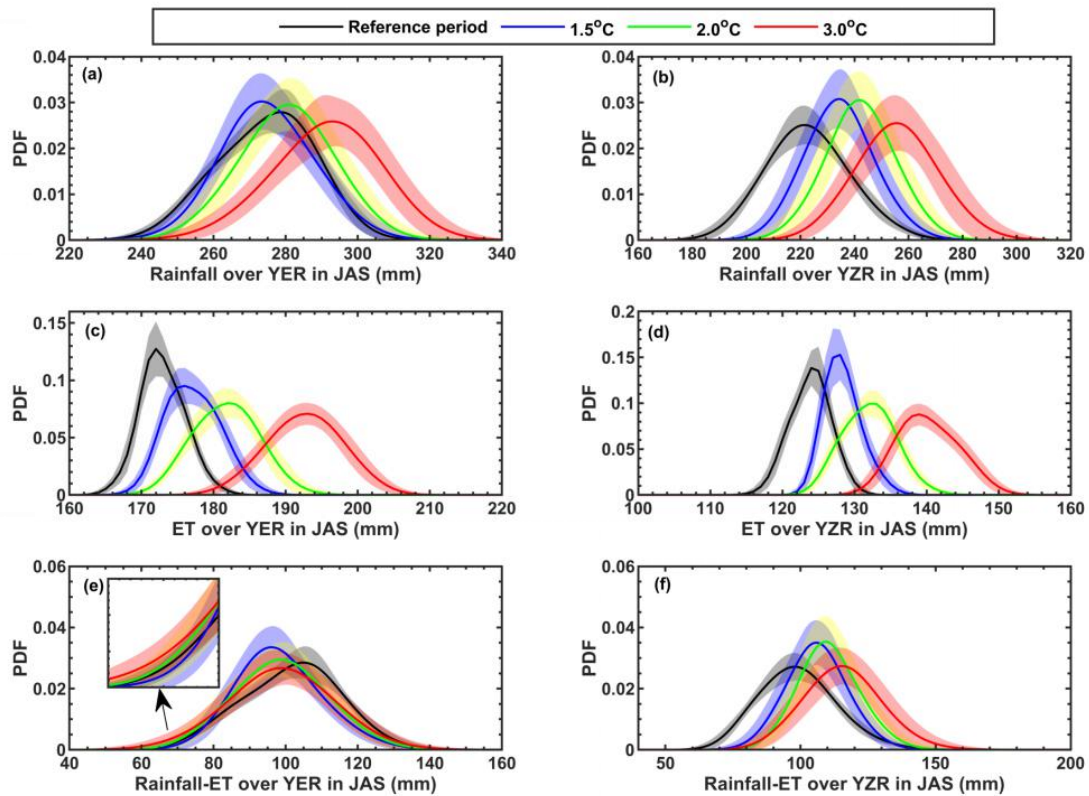
687 Solid lines represent ensemble means, while shadings are ranges of individual

688 ensemble members. (b) Percent changes in frequency of dry and wet extremes in

689 July-September at different warming levels. Colored bars are ensemble means, while

690 error bars are 5~95% uncertainty ranges estimated by using bootstrapping for 10,000

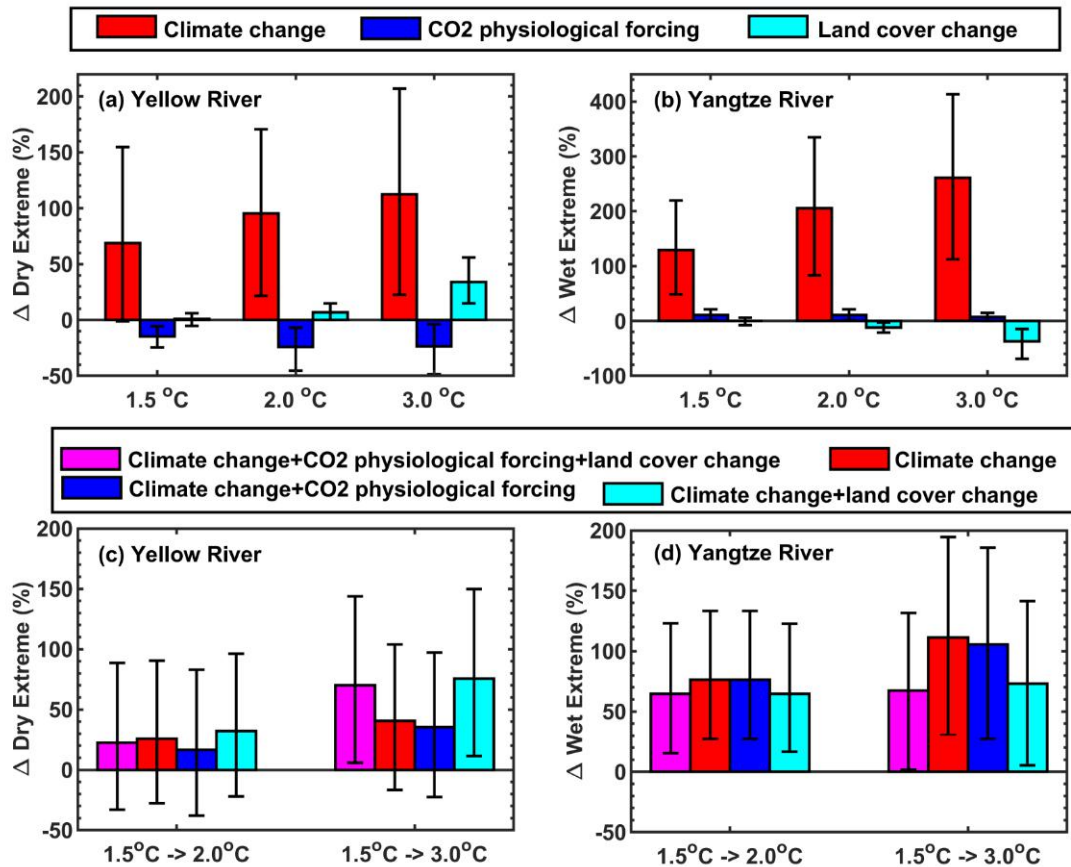
691 times. (c) and (d) are the same as (a) and (b), but for the Yangtze river.



693

694 **Figure 6.** Probability density functions (PDFs) of regional mean rainfall,
 695 evapotranspiration (ET) and their difference over the headwater regions of Yellow
 696 river (YER) and Yangtze river (YZR) during flooding seasons (July-September) for
 697 the reference period (1985-2014) and the periods with 1.5, 2.0 and 3.0°C global
 698 warming levels. Shadings are 5~95% uncertainty ranges.

699



700

701 **Figure 7.** (a-b) Influences of climate change, CO₂ physiological forcing and land

702 cover change on relative changes in frequency of the dry and wet extremes in

703 July-September at different global warming levels for the headwater regions of

704 Yellow river and Yangtze river. (c-d) Changes of dry and wet extremes under

705 additional warming of 0.5 °C and 1.5 °C with the consideration of different factors. All

706 the changes are relative to the reference period (1985-2014). Ensemble means are

707 shown by colored bars while the 5~95% uncertainty ranges estimated by using

708 bootstrapping for 10,000 times are represented by error bars.

709

710 **Table 1.** CMIP6 simulations used in this study. His means historical simulations
711 during 1979-2014 with both anthropogenic and natural forcings, SSP245 and SSP585
712 represent two Shared Socioeconomic Pathways during 2015-2100. Note the
713 CNRM-CM6-1 and CNRM-ESM2-1 do not provide r1ilp1f1 realization, so r1ilp1f2
714 was used instead.

No.	Models	Experiments	Realization	Horizontal Resolution (Longitude × Latitude Grid Points)
1	ACCESS-ESM1-5	His/SSP245/SSP585	r1ilp1f1	192×145
2	BCC-CSM2-MR	His/SSP245/SSP585	r1ilp1f1	320×160
3	CESM2	His/SSP245/SSP585	r1ilp1f1	288×192
4	CNRM-CM6-1	His/SSP245/SSP585	r1ilp1f2	256×128
5	CNRM-ESM2-1	His/SSP245/SSP585	r1ilp1f2	256×128
6	EC-Earth3-Veg	His/SSP245/SSP585	r1ilp1f1	512×256
7	FGOALS-g3	His/SSP245/SSP585	r1ilp1f1	180×80
8	GFDL-CM4	His/SSP245/SSP585	r1ilp1f1	288×180
9	INM-CM5-0	His/SSP245/SSP585	r1ilp1f1	180×120
10	MPI-ESM1-2-HR	His/SSP245/SSP585	r1ilp1f1	384×192
11	MRI-ESM2-0	His/SSP245/SSP585	r1ilp1f1	320×160

715

716 **Table 2.** Determination of “crossing years” for the periods reaching 1.5, 2 and 3°C
 717 warming levels for different GCM and SSP combinations.

Models	1.5°C warming level		2.0°C warming level		3.0°C warming level	
	SSP245	SSP585	SSP245	SSP585	SSP245	SSP585
ACCESS-ESM1-5	2024	2023	2037	2034	2070	2052
BCC-CSM2-MR	2026	2023	2043	2034	Not found	2054
CESM2	2024	2022	2037	2032	2069	2048
CNRM-CM6-1	2032	2028	2047	2039	2075	2055
CNRM-ESM2-1	2030	2026	2049	2039	2075	2058
EC-Earth3-Veg	2028	2023	2044	2035	2072	2053
FGOALS-g3	2033	2032	2063	2046	Not found	2069
GFDL-CM4	2025	2024	2038	2036	2073	2053
INM-CM5-0	2031	2027	2059	2038	Not found	2063
MPI-ESM1-2-HR	2032	2030	2055	2044	Not found	2066
MRI-ESM2-0	2024	2021	2038	2030	2074	2051

718

719 **Table 3.** Performance for CSSPv2 model simulations driven by the observed
720 meteorological forcing (CMFD/CSSPv2) and the bias-corrected CMIP6 historical
721 simulations (CMIP6_His/CSSPv2). The metrics include correlation coefficient (CC),
722 root mean squared error (RMSE), and Kling-Gupta efficiency (KGE). The KGE is
723 only used to evaluate streamflow.

Variables	Experiments	CC	RMSE	KGE
Monthly streamflow at TNH station	CMFD/CSSPv2	0.95	165 m ³ /s	0.94
	CMIP6_His/CSSPv2	0.76	342 m ³ /s	0.71
Monthly streamflow at ZMD station	CMFD/CSSPv2	0.93	169 m ³ /s	0.91
	CMIP6_His/CSSPv2	0.82	257 m ³ /s	0.81
Monthly terrestrial water storage anomaly over the Sanjiangyuan region	CMFD/CSSPv2	0.7	22 mm/month	-
	CMIP6_His/CSSPv2	0.4	24 mm/month	-
Annual evapotranspiration over the Sanjiangyuan region	CMFD/CSSPv2	0.87	14 mm/year	-
	CMIP6_His/CSSPv2	0.47	13 mm/year	-

724

725